Supplemental material for "**Rank-One Prior: Toward Real-Time Scene Recovery**"

Jun Liu, Ryan Wen Liu, Jianing Sun, Tieyong Zeng
{liuj292,sunjn118}@nenu.edu.cn, wenliu@whut.edu.cn, zeng@math.cuhk.edu.hk

I. Overview

This supplemental material provides more experiments of sandstorm/underwater image/video enhancement and image/video dehazing for a better illustration of our method [1].

II. More Results

A. Derivation of equation (7)

The transmission $\tilde{t} = \mathbf{C}\mathbf{S}_{nu}$ is obtained by solving:

$$\mathbf{C} = \arg\min_{\mathbf{C}} \|\mathbf{I} - \tilde{t}\|^2 = \arg\min_{\mathbf{C}} \|\mathbf{I} - \mathbf{C}\mathbf{S}_{nu}\|^2 = \langle \mathbf{I}, \mathbf{S}_{nu} \rangle$$

i.e., $\tilde{t} = \langle \mathbf{I}, \mathbf{S}_{nu} \rangle \cdot \mathbf{S}_{nu}$, which means that $\tilde{t}$ is the projection of $\mathbf{I}$ along the direction $\mathbf{S}_{nu}$. This is equation (7).

B. Numerical results

In this subsection, we give more visual comparisons among different methods for different applications. We compare our method with ten state-of-the-art enhancing/dehazing methods. Specifically, Li et al. [1] proposed the atmosphere scattering model and an AOD-Net to estimate clear images. Ren et al. [2] proposed a multi-scale deep neural network for single-image dehazing by learning the mapping between hazy images and their corresponding transmission maps. He et al. [3] proposed a dark channel prior (DCP) based on the statistics of haze-free images. This method is based on a key observation that most local patches in haze-free outdoor images contain some pixels which have very low intensities in at least one color channel. Zhu et al. [4] proposed a fusion of luminance and dark channel prior (F-LDCP) method to effectively restore long-shot images naturally, especially for the sky region. Berman et al. [5] proposed a new method for calculating the air-light. This method relies on the haze-lines prior [6]. For underwater image enhancement, Fu et al. [7] proposed a retinex-based method including three steps to solve three subproblems for the color correction, the reflectance and the illumination decomposition, the reflectance and the illumination enhancement, respectively. Their method is also effective for sandstorm image enhancement. In [8], Fu et al. further proposed a two-step approach by correcting color shift firstly and addressing low contrast at last. Li et al. [9] proposed a systematic underwater image enhancement method with minimum information Loss and histogram distribution prior. Peng et al. [10] proposed a depth estimation method for underwater scenes based on image blurriness and light absorption. For the sandstorm image enhancement, Fu et al. [11] proposed a fusion-based method which can overcome the color distortion, low-visibility, fuzz and non-uniform luminance.

Fig. 1 shows the sandstorm image enhancement results obtained by different methods. This comparison confirms our superiority in sandstorm image enhancement. The superior imaging performance can be also further confirmed by the video enhancement results shown in Fig. 2. For the underwater image enhancement, the results are shown in Fig. 3. The image dehazing results obtained by different methods are shown in Fig. 4 and Fig. 5. As can be seen from the results of the comparison, our method has much more stable performance in different applications.

Video dehazing results by different methods is shown in Fig. 6. We observe that LDCP [4] can produce much brighter results than DCP [12], MSCNN [2], and AODNet [1]. However, LDCP is not stable since it changes the saturation in different frames. In comparison, our method is more stable and produces better results.

Note that one novel work 'Non-local image dehazing' (NLD)[6] can provides good results on dehazing. This method is based on the observations: 1) distinct colors in a haze-free image are usually clustered discretely in the RGB colorspace; 2) for the hazy image, the pixels in a given cluster are in generally non-local and are spread over the entire image plane. Those color clusters form a "haze-line", and the position of a pixel within the line reflects its transmission level. Consequently, these haze-lines can be used to estimate the transmission map. Fig. 7 shows the comparison of non-local dehazing and ours. We can observation that NLD can provide a good dehazing result for some haze image, e.g., the last row, while our method is less effective. We will further propose an improved version of our method which can have more effective dehazing performance.

[1]This file is a reduced size PDF. The quality of images may be affected. The reader can contact the authors to obtain the full-size PDF.

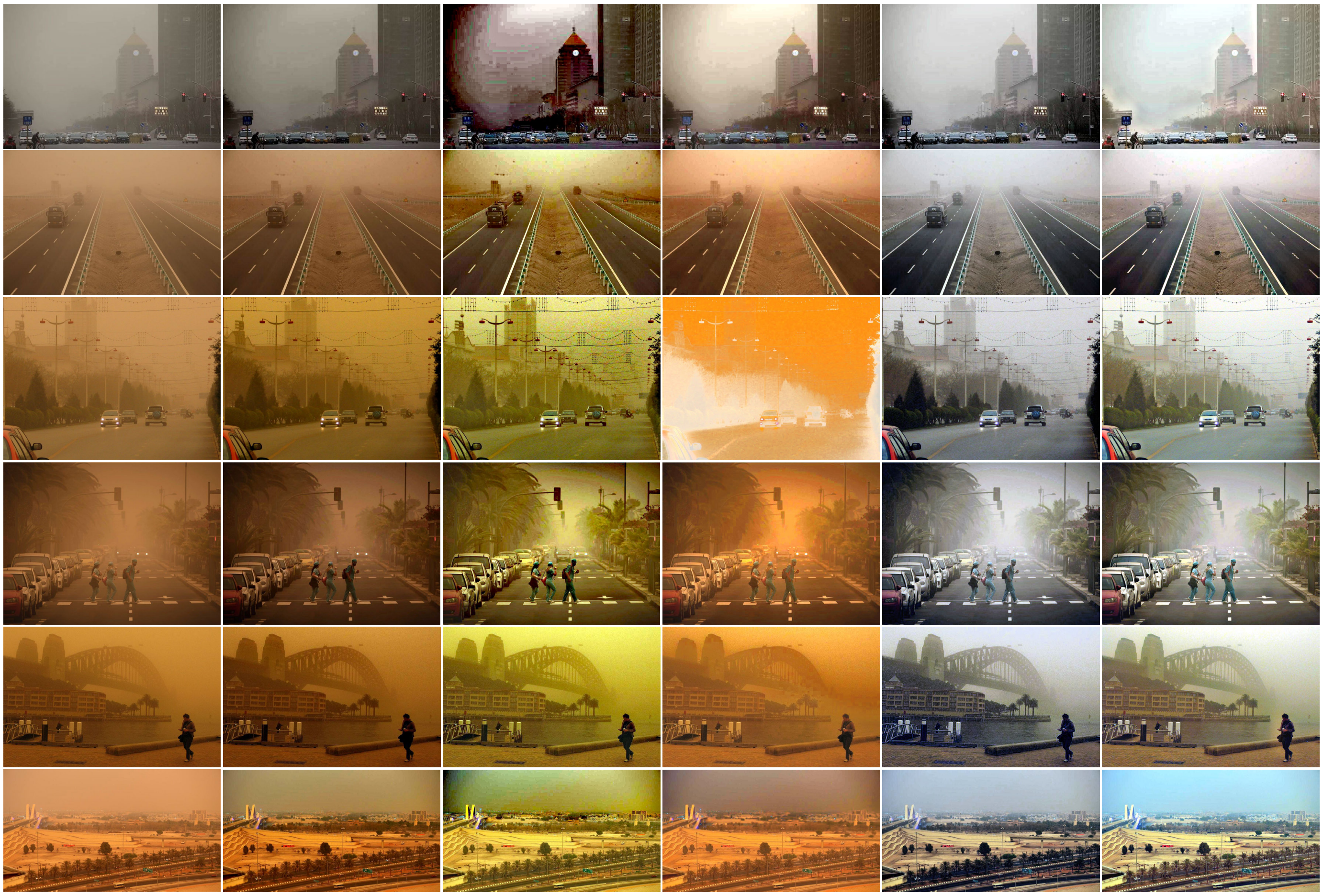

(a) Raw images (c) MSCNN [2] (d) Haze-Lines [5] (e) LDCP [4] (f) Fusion [11] (h) Ours

Fig. 1: Sandstorm image enhancement results obtained by different methods. (The images are best viewed in the full-screen mode.)

(a) Frame 1 (b) Frame 5 (c) Frame 9 (d) Frame 13 (e) Frame 17 (f) Frame 21 (g) Frame 25 (h) Frame 29

Fig. 2: Sandstorm video enhancement results obtained by different methods. First row presents the input frames; second row is the corresponding enhanced results by Fu et al.'s method [7]; third row is the results by our method. (The images are best viewed in the full-screen mode.)

References

[1] B. Li, X. Peng, Z. Wang, J. Xu, and D. Feng, "Aod-net: All-in-one dehazing network," in *Proceedings of the IEEE International Conference on Computer Vision*, 2017, pp. 4770–4778.

[2] W. Ren, S. Liu, H. Zhang, J. Pan, X. Cao, and M.-H. Yang, "Single image dehazing via multi-scale convolutional neural networks," in *Proceedings of the European Conference on Computer Vision (ECCV)*. Springer, 2016, pp. 154–169.

[3] K. He, J. Sun, and X. Tang, "Single image haze removal using dark channel prior," in *Proceedings of the IEEE Conference on Computer Vision and Pattern Recognition*, vol. 1, 2009, pp. 1956–1963.

[4] Y. Zhu, G. Tang, X. Zhang, J. Jiang, and Q. Tian, "Haze removal method for natural restoration of images with sky," *Neurocomputing*, vol. 275, pp. 499–510, 2018.

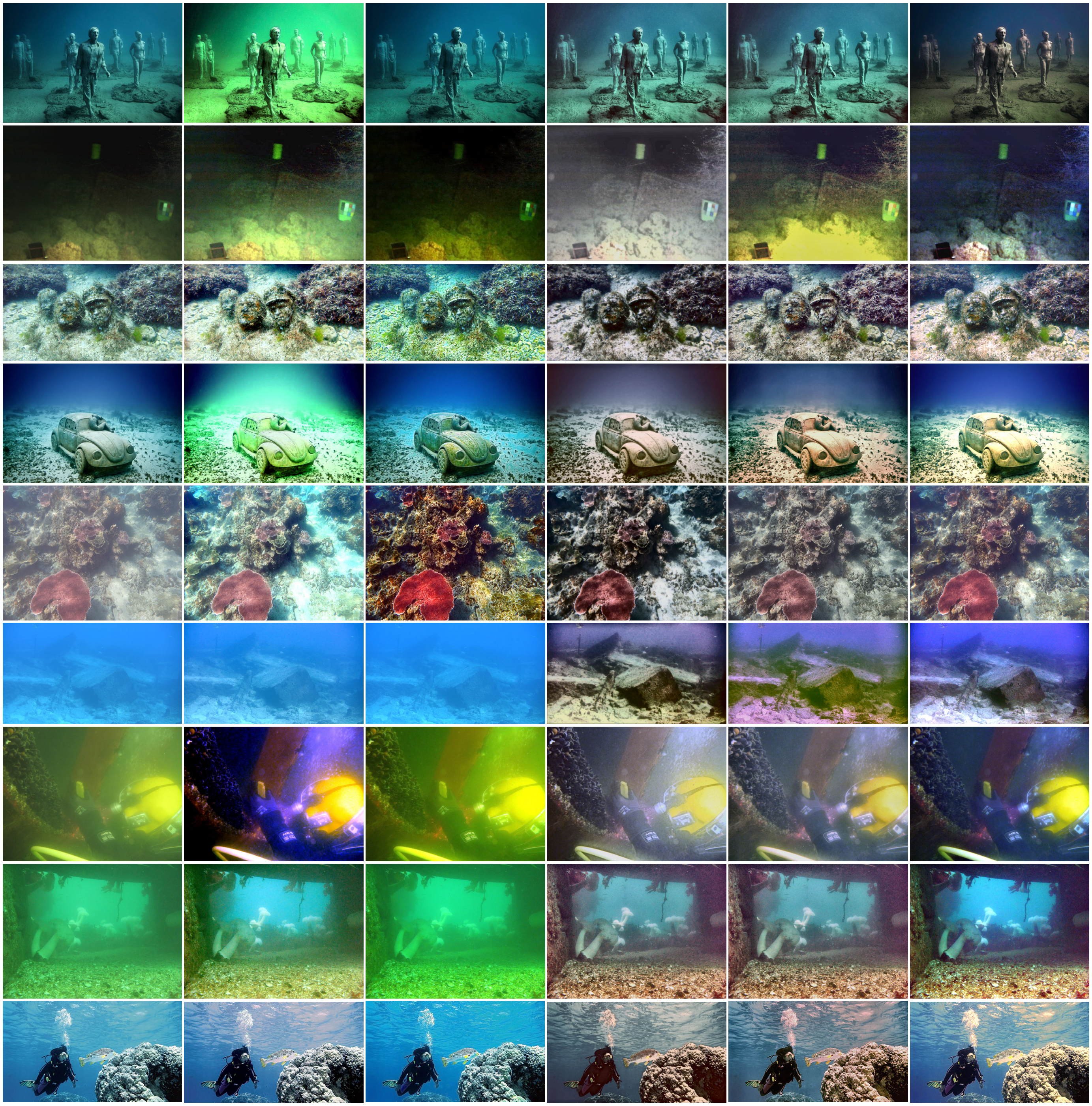

(a) Raw images (b) Blurriness [10] (c) histogram prior [9] (d) Retinex [7] (e) Two-step [8] (f) Ours

Fig. 3: Dehazing results obtained by different methods. (The images are best viewed in the full-screen mode.)

[5] D. Berman, T. Treibitz, and S. Avidan, "Air-light estimation using haze-lines," in *2017 IEEE International Conference on Computational Photography (ICCP)*, 2017, pp. 1–9.

[6] D. Berman, S. Avidan *et al.*, "Non-local image dehazing," in *Proceedings of the IEEE conference on Computer Vision and Pattern Recognition*, 2016, pp. 1674–1682.

[7] X. Fu, P. Zhuang, Y. Huang, Y. Liao, X.-P. Zhang, and X. Ding, "A retinex-based enhancing approach for single underwater image," in *2014 IEEE International Conference on Image Processing (ICIP)*, 2014, pp. 4572–4576.

[8] X. Fu, Z. Fan, M. Ling, Y. Huang, and X. Ding, "Two-step approach for single underwater image enhancement," in *2017 International Symposium on Intelligent Signal Processing and Communication Systems (ISPACS)*, 2017, pp. 789–794.

[9] C.-Y. Li, J.-C. Guo, R.-M. Cong, Y.-W. Pang, and B. Wang, "Underwater image enhancement by dehazing with minimum information loss and histogram distribution prior," *IEEE Transactions on Image Processing*, vol. 25, no. 12, pp. 5664–5677, 2016.

[10] Y.-T. Peng and P. C. Cosman, "Underwater image restoration based on image blurriness and light absorption," *IEEE Transactions on Image Processing*, vol. 26, no. 4, pp. 1579–1594, 2017.

(a) Raw images (b) DCP [12] (c) MSCNN [2] (d) LDCP [4] (e) AODNet [1] (e) Ours

Fig. 4: Dehazing results obtained by different methods. (The images are best viewed in the full-screen mode.)

[11] X. Fu, Y. Huang, D. Zeng, X.-P. Zhang, and X. Ding, “A fusion-based enhancing approach for single sandstorm image,” in *2014 IEEE 16th International Workshop on Multimedia Signal Processing (MMSP)*, 2014, pp. 1–5.

[12] K. He, J. Sun, and X. Tang, “Single image haze removal using dark channel prior,” *IEEE Transactions on Pattern Analysis and Machine Intelligence*, vol. 33, no. 12, pp. 2341–2353, 2010.

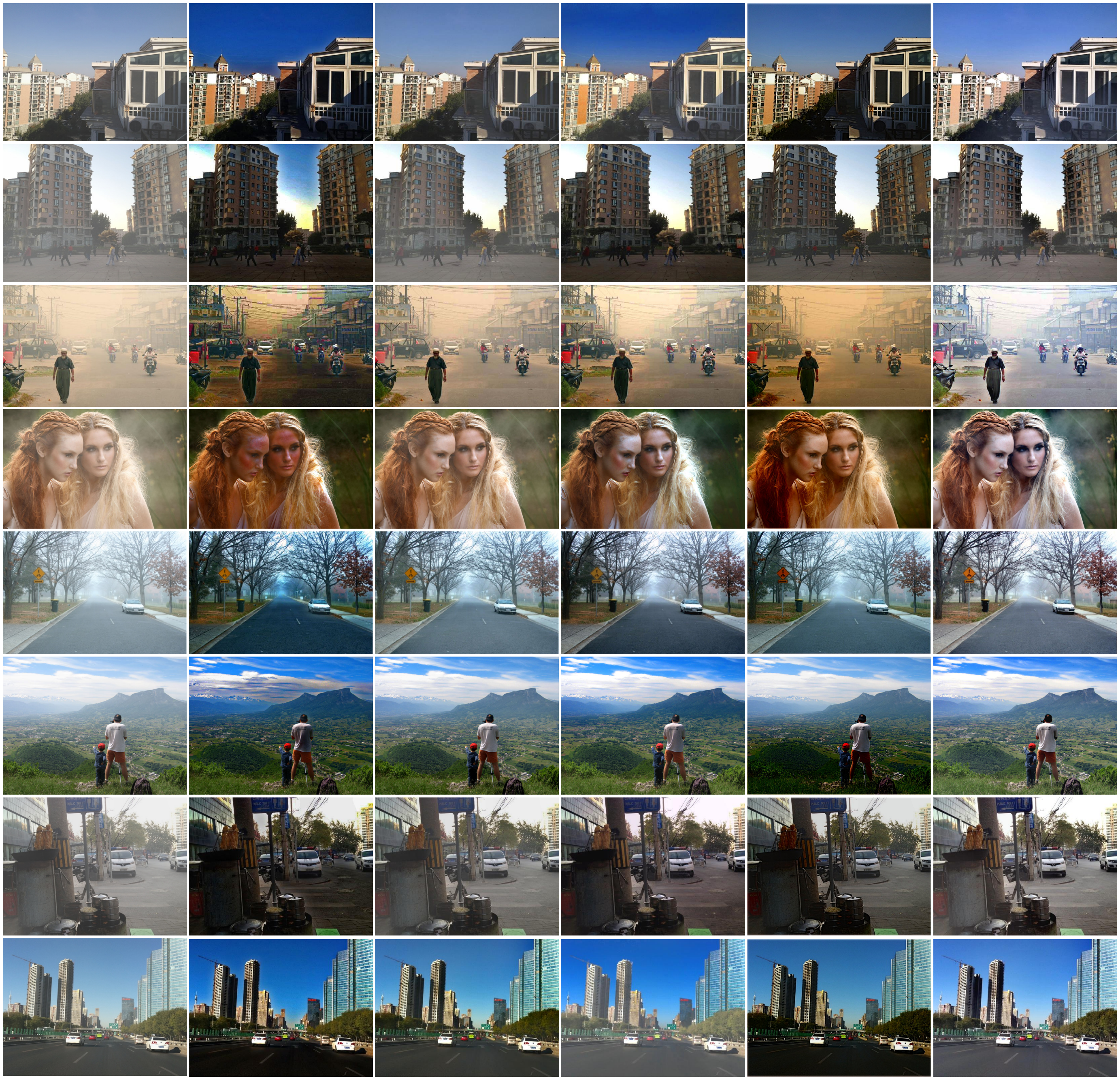

(a) Raw images (b) DCP [12] (c) MSCNN [2] (d) LDCP [4] (e) AODNet [1] (f) Ours

Fig. 5: Dehazing results obtained by different methods. (The images are best viewed in the full-screen mode.)

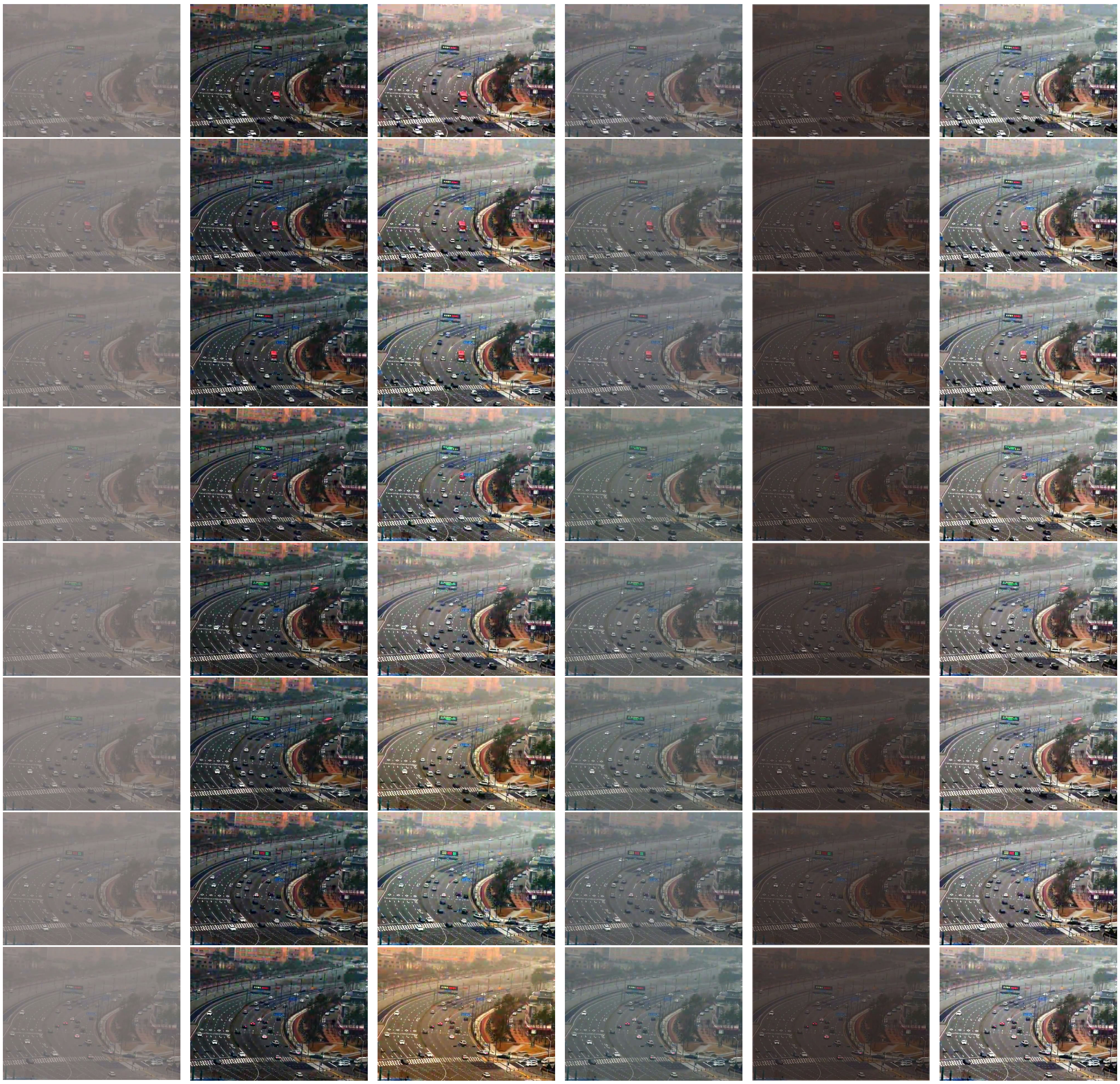

(a) Input (b) DCP [12] (c) LDCP [4] (d) MSCNN [2] (e) AODNet [1] (f) Ours

Fig. 6: Video dehazing results obtained by different methods. (The images are best viewed in the full-screen mode.)

(a) Hazy image (b) Ours (c) Non-local dehazing

Fig. 7: Dehazing performance in comparison with the non-local dehazing method [6]. (The images are best viewed in the full-screen mode.)